

# Metabolic constraints on the body size scaling of extreme population densities

Angel Segura<sup>1</sup> and Gonzalo Perera<sup>2</sup>

<sup>1</sup>Facultad de Ciencias

<sup>2</sup>Universidad de la República, Centro Universitario Regional Este, Modelización y Análisis de Recursos Naturales, Uruguay

November 29, 2022

## Abstract

Pest outbreaks, harmful algal blooms, and population collapses are extreme events with critical consequences for ecosystems, highlighting the importance of deciphering the driving ecological mechanisms underlying extreme events. By combining the generalized extreme value (GEV) theory from statistics and the hypothesis of a resource-limited metabolic restriction to population abundance, we evaluated theoretical predictions on the size-scaling and variance of extreme population abundance. Phytoplankton data from the L4 station in the English Channel showed a negative size scaling of the expected value of maxima, whose confidence interval included the predicted metabolic scaling ( $\alpha = -1$ ). We showed a humped pattern in variance with maxima at intermediate sizes. These results are consistent with the bounded abundance of small-sized populations that are subjected to strong grazing and with the expected decrease in variance towards large sizes. This approach provides unbiased return times, thereby improving the prediction accuracy of the timing of bloom formation, and describes a coherent framework in which to explore extreme population densities in natural communities.

1 Metabolic constraints on the body size scaling of extreme population densities

2

3 Segura A.M.<sup>1\*</sup> & Perera, G.<sup>1,2</sup>

4 <sup>1</sup> Modelización Estadística de Datos e Inteligencia Artificial (MEDIA), Centro Universitario

5 Regional del Este, Universidad de la República, Rocha, Uruguay.

6 <sup>2</sup> Instituto de Matemática y Estadística Rafael Laguarda (IMERL), Facultad de Ingeniería,

7 Universidad de la República

8

9 To be submitted to: Ecology letters

10 \*Corresponding author

11 Angel M. Segura

12 e-mail: [asegura@cure.edu.uy](mailto:asegura@cure.edu.uy)

13 CURE-Rocha, Ruta 9 km 210. PC 27000

14 Type= Letter

**# of words: 3684 in abstract: 147**

**# Figures: 4**

**# Citations: 44**

15 **Author`s contribution:** AMS designed research, generate R codes and results and write a first  
16 draft. GP provided analytical tools and contributed to the writing of the final draft.

**Data accessibility statement:**

Should the manuscript be accepted, the data supporting the results will be archived in Zenodo and the code for downloading and analyzing data will be deposited in the same repository. It will be available i) the raw data files that were analyzed to produce the statistics and figures reported in the paper, ii) a metadata file explaining what the data are in each column and what rows represent. The units of measurement and a verbal description in English of the data included in each column, iii) the computer code used to produce the figures in R. Station L4 data are archived at the British Oceanographic Data Centre [www.bodc.ac.uk](http://www.bodc.ac.uk) under DOI:10.5285/c9386b5c-b459-782f-e053-

6c86abc0d129and are freely available at  
[https://www.bodc.ac.uk/data/published\\_data\\_library/catalogue/10.5285/c9386b5c-b459-782f-e053-6c86abc0d129/](https://www.bodc.ac.uk/data/published_data_library/catalogue/10.5285/c9386b5c-b459-782f-e053-6c86abc0d129/). Western Channel Observatory (L4) nutrient concentration profiles (2000 – 2020)  
doi:10.5285/bc3cf5ce-d18c-1f42-e053-6c86abc02e29

17 **Abstract**

18 Pest outbreaks, harmful algal blooms, and population collapses are extreme events with critical  
19 consequences for ecosystems, highlighting the importance of deciphering the driving ecological  
20 mechanisms underlying extreme events. By combining the generalized extreme value (GEV) theory  
21 from statistics and the hypothesis of a resource-limited metabolic restriction to population  
22 abundance, we evaluated theoretical predictions on the size-scaling and variance of extreme  
23 population abundance. Phytoplankton data from the L4 station in the English Channel showed a  
24 negative size scaling of the expected value of maxima, whose confidence interval included the  
25 predicted metabolic scaling ( $\alpha=-1$ ) and a humped pattern in variance. These results are consistent  
26 with the bounded abundance of small-sized populations that are subjected to strong grazing and  
27 with the expected decrease in variance towards large sizes. This approach provides unbiased return  
28 times, thereby improving the prediction accuracy of the timing of bloom formation under a coherent  
29 framework.

30

31 **Keywords:** Extreme events, generalized extreme value distribution, metabolic limit, scaling

## 32 INTRODUCTION

33 Extreme events are relevant for ecosystem functioning in terms of both the impact of abiotic  
34 extremes in the abundance of natural populations (*e.g.*, hurricanes, tsunamis) and in the extremes  
35 caused by intrinsic population dynamics (May 1973; Bjornstad 2001). Species collapse, pest  
36 outbreaks, and harmful algal blooms are pertinent examples of events with important consequences  
37 for the environment, human health, and conservation. Descriptions of the dynamics of extreme  
38 events in hydrology date back to the early eighteenth century; today, a statistical theory of extreme  
39 values is well developed (*e.g.* Embrechts *et al.* 2008). For decades, extreme environmental effects  
40 have been of interest to both population and community ecology (Gaines & Denny 1993; Katz *et al.*  
41 2005), and more recent studies have advanced our understanding of the distribution of extreme  
42 population dynamics (Segura *et al.* 2013; Batt *et al.* 2017). However, there continues to lack a  
43 formal test of the mechanisms driving the limits of extreme population abundances. Two aspects  
44 deserve special attention; first, GEV distribution provides an unbiased estimation of return period of  
45 extreme events. This is critical to predict the timing of population outbursts, because the use  
46 classical distributions (*e.g.*, Gaussian) could lead to a large underestimation of the average time  
47 between extreme population's abundance (*i.e.* return times, Fig. 1). This bias could lead to wrong  
48 management actions, or the sense of unpredictability of the extreme events. Second, the analysis of  
49 extremes is conceptually rooted on defining an upper limit to abundance in populations or  
50 communities, but the theoretical basis is not well developed (Lawton 1989; Barneche *et al.* 2016).

51         The limits to maximum population abundance are set by the ability of a population to  
52 transform resources into offspring and minimize losses, while embedded in a complex network of  
53 interactions (Lawton 1989; Bjornstad 2001). Macroscopic approaches are useful to understand the  
54 structure and dynamics of ecosystems because they simplify the complexity of natural systems by  
55 describing a set of general patterns using observable variables (*e.g.* body volume) linked by power  
56 scaling laws (Brown *et al.* 2004; Marquet 2005). Body size is related to metabolism, growth,

57 abundance, and predator defence, among other processes and it is considered a master trait in  
58 ecology (Brown *et al.* 2004; Zaoli *et al.* 2017; Hatton *et al.* 2019). The metabolic limit to maximum  
59 population abundances depends on body size, and this relationship has been suggested as a  
60 macroscopic approach to this problem (Agustí *et al.* 1987; Belgrano *et al.* 2002; Deng *et al.* 2012).

61 The formal link between the scaling of population abundances with body size and extreme  
62 value theory provides a fruitful avenue to explore metabolic limits of extreme population  
63 abundances in natural communities. In the present paper, under the hypothesis of a metabolic  
64 restriction to maximum populations abundance, we developed a theoretical model and tested  
65 specific formal predictions on the distribution of extreme population abundances using one of the  
66 most comprehensive time series of abundance in a natural community.

67

## 68 **Model formulation**

### 69 *Metabolic limits to maximum population abundance*

70 Without loss of generality, we developed a theoretical model for aquatic primary producers;  
71 however, the principles and formulations are generalizable to other ecosystems and taxonomic  
72 groups. The size density relationship (SDR) presents a power law relationship between body-size  
73 ( $M$ ) and maximum population density  $max(N)$  (Belgrano *et al.* 2002; Brown *et al.* 2004; Barneche  
74 *et al.* 2016; Segura & Perera 2019):

$$75 \quad max(N) = a M^{-\alpha} \quad (1)$$

76 where the power  $\alpha$  is the scaling of the metabolic rate and body size and  $a$  is a temperature and  
77 resource normalization constant. This relationship is based on the assumption that total resource use  
78 ( $R_{tot}$ ) in a local ecosystem (e.g., light or nutrients in the case of autotrophs) is equal to the sum of  
79 the population-level rates of resource use per unit area or volume,  $R_i$ , across  $S$  cohabiting species.

80  $R_i$ , in turn, is proportional to the product of the metabolic rate ( $B_i$ ) and the population density per  
 81 unit area or volume ( $N_i$ ):

$$82 \quad R_i = N_i B_i \quad (2)$$

83 Our interest is in understanding the upper limit to population density,  $\max(N_i)$ . Assuming a  
 84 dominant species can use no more than  $\gamma$  of total resources ( $R_{tot}$ ) and that metabolic rate is a  
 85 function of body size and temperature (Brown *et al.* 2004)

$$86 \quad B_i = b_0 e^{\frac{-E}{kT}} M_i^\alpha \quad (3)$$

87 Where  $b_0$  is a taxon-dependent normalization constant,  $E$  is the activation energy (eV) and  $k$  is the  
 88 Boltzmann constant ( $1.6 \times 10^{-5}$  eVK<sup>-1</sup>). Replacing eq. 3 in eq. 2, and then substituting  $\gamma R_{tot}$  for  $R_i$ , it  
 89 is possible to explore the relationship for maximum population density (Belgrano *et al.* 2002; Deng  
 90 *et al.* 2012):

$$91 \quad \max(N_i) = \gamma b_0^{-1} R_{tot} e^{\frac{E}{kT}} M_i^{-\alpha} \quad (4)$$

92 Taking the logarithm in both sides, following Segura and Perera (2019), we can define:

$$93 \quad n_{max} = \log(\max(N_i)) = [\log(\gamma) + \log(b_0^{-1}) + \log(R_{tot}) + \frac{E}{kT}] - \alpha \log(M_i) \quad (5)$$

94 Here, we explore the role of nutrients in the fraction of resources used by dominant species by  
 95 assuming that  $\gamma$  is resource- and size-dependent  $\gamma = f(R_{tot}, M)$  and bounded between 0 and 1. The  
 96 size-dependent fraction of total resources captured by a given dominant species can be modelled as  
 97 a Monod-like function (Huisman *et al.* 1999):

$$98 \quad \gamma \propto \frac{R_{tot}}{R_{tot} + k_s} \quad (6)$$

99 where  $k_s$  is the half saturation constant.

100 Two resources are fundamental for primary producers, nutrients, and light. The  
 101 concentration of dissolved inorganic nitrogen (DIN) forms, which is the sum of nitrate (NO<sub>3</sub>), nitrite  
 102 (NO<sub>2</sub>), and ammonia (NH<sub>4</sub>), are limiting in marine ecosystems and theoretical biophysical  
 103 arguments on the dynamics of exchange of resources across the cell membrane suggest a specific  
 104 size-scaling of  $k_s$  ( $k_s \sim M^{0.33}$ ) (Aksnes & Egge 1991). In the case of phytoplankton, an empirical  
 105 power law scaling with body size supporting this biophysical theoretical model has been found ( $k_s =$   
 106  $0.14 M^{0.33}$ ; Edwards *et al.* 2012). Light limitation is a complex process but exhibits a saturating  
 107 curve with respect to light, and it has been modelled using a Monod formulation with an invariant  
 108 half saturation constant ( $k_{PAR} = 1.51 \text{ mol photons m}^{-2} \text{ day}^{-1}$ ) in phytoplankton (Huisman *et al.* 1999;  
 109 López-Urrutia *et al.* 2006). Under steady state, metabolism is limited by the most limiting rate  
 110 (dictated by nutrients or light); therefore, we define a general  $k_R$  that represents either nutrient or  
 111 light limitation. Including the theoretical formulation for the fraction of resources used by dominant  
 112 species (eq. 6) into eq. 5:

$$113 \quad n_{max} = \log(\max(N_i)) = \left[ \log\left(\frac{R_{tot}}{R_{tot} + k_R}\right) + \log(b_0^{-1}) + \log(R_{tot}) + \frac{E}{kT} \right] - \alpha \log(M_i) \quad (7)$$

114 Equation 7 allows the generation of testable predictions about the relationship between size,  
 115 resources, temperature, and extreme population abundance.

### 116 *The generalized extreme value theory*

117 Taking the maximum of a finite sequence of independent and identically distributed (*iid*) random  
 118 variables leads to an asymptotic distribution satisfying the “max-stability property” (Katz *et al.*  
 119 2005; Embrechts *et al.* 2008). There are three nominal distributions of extreme values, namely, the  
 120 Weibull, Gumbel, and Fréchet distributions. They result from taking maxima from *iid* bounded  
 121 (*e.g.*, Uniform), unbounded with light tailed (*e.g.*, Gaussian), and unbounded with fat-tailed (*e.g.*,  
 122 Cauchy) distributions. The general extreme value (GEV) distribution is a family of continuous  
 123 probability distributions, which includes the three mentioned canonical extremal distributions. Its  
 124 cumulative function (F) is described as:

$$F(x, \mu, \sigma, \xi) = \begin{cases} \exp\{-[1 + \xi(x - \mu)/\sigma]^{-1/\xi}\}, & 1 + \xi(x - \mu)/\sigma > 0, \quad \xi \neq 0 \\ \exp\{-\exp(-(x - \mu)/\sigma)\}, & \xi = 0 \\ 0, & \xi(x - \mu)/\sigma \leq -1, \quad \xi > 0 \\ 1, & \xi(x - \mu)/\sigma \leq -1, \quad \xi < 0 \end{cases} \quad (8)$$

126 Where  $\mu$  is the location,  $\sigma > 0$  is the scale, and  $\xi$  is a shape parameter. The location specifies the  
 127 centre of the distribution, the scale is the spread, and the shape is a relevant parameter that describes  
 128 the behaviour of the tails. The shape parameter ( $\xi$ ) is critical to understand ecological dynamics, as  
 129 it characterizes whether the distribution of maxima is bounded (*i.e.*  $\xi < 0$ ), has a light tail (*i.e.*  $\xi =$   
 130  $0$ ), or has a heavy tail (*i.e.*,  $\xi > 0$ ). There are many ecological mechanisms that can drive the  
 131 outburst of species abundance and, thus heavy tailed extremal distributions ( $\xi > 0$ ), as suggested by  
 132 previous analysis (Keitt & Stanley 1998; Segura *et al.* 2013; Batt *et al.* 2017), but other ecological  
 133 mechanisms may keep populations constrained within a bounded range of abundances (Bjornstad  
 134 2001; Segura *et al.* 2013).

135 From the metabolic dependence of maximum population density (eqs. 4 and 7) we derive a set of  
 136 specific predictions amenable to testing under the GEV theory. The size-scaling of the expected  
 137 valued of the GEV will match the scaling of metabolism ( $\alpha$ ), which in marine phytoplankton was  
 138 found empirically to be one ( $\alpha=1$ ; López-Urrutia *et al.* (2006)). The variance of population  
 139 fluctuations will decrease with body size (Segura & Perera 2019). However, a strong match of  
 140 populations abundance driven by predation (as it occurs in the lower size fractions in  
 141 phytoplankton) will exhibit deviations from this pattern. Using the SDR framework and the GEV  
 142 theory, we test explicit predictions using one of the longest time series of abundance in a species-  
 143 rich community of plankton in the English Channel L4 station.

144

## 145 **MATERIALS AND METHODS**

### 146 *Time series description*

147 Phytoplankton abundance and individual volume information were obtained from data collected in

148 the Western English Channel, 10 nautical miles off Plymouth (50°15' N, 4°13' W), at the L4 station  
149 and provided by the Western Channel Observatory  
150 (<http://www.westernchannelobservatory.org.uk/l4/Phytoplankton>) (Widdicombe & Harbour 2021).

151 This is an extensive data set of more than 200 species and consisted of 28 years' worth (October  
152 1992 to June 2020) of weekly sampled phytoplankton abundance (N weeks = 1183). Some weeks  
153 were not sampled due to weather issues. Detailed information on sampling design, taxonomic  
154 identification and counting methodologies can be found in Widdicombe *et al.* (2010) and  
155 Widdicombe and Harbour (2021). Average individual volume ( $\mu\text{m}^3/\text{org}$ ) was used as a proxy for  
156 body size.

157 Temperature was measured *in situ* using CTD. Water samples were kept refrigerated until nutrient  
158 concentration ( $\mu\text{M}$ ) was analysed using a 5-channel Bran and Luebbe segmented flow colorimetric  
159 autoanalyser (Norderstedt, Germany) (Woodward & Harris 2021). Dissolved inorganic nitrogen  
160 (DIN) is defined as the sum of the nitrate, nitrite, and ammonia concentrations ( $\text{NO}_3$ ,  $\text{NO}_2$ , and  $\text{NH}_4$ )  
161 and provide an estimate of the generally limiting resource in the L4 station (Smyth *et al.* 2010).  
162 Dissolved inorganic nitrogen concentrations below the half saturation constant ( $k_s$ ) were defined as  
163 limiting. As the saturation constant was defined to scale allometrically, each phytoplankton size  
164 class exhibited a different limitation threshold. The fraction of weeks where DIN was below  $k_s$  was  
165 calculated for each phytoplankton size class.

#### 166 *Parameter estimation*

167 Phytoplankton populations were combined in size bins (in  $\log_2$ ) classes from 5 to 19 every two units  
168 ( $\log_2(\mu\text{m}^3 \text{ org}^{-1})$ ) (Segura *et al.* 2011), and for each bin we estimated maximum population  
169 abundance every week. Maximum population abundance per week was estimated for an average of  
170 27 species per size-bin.

171 We employed two complementary approaches to evaluate theoretical predictions on the size scaling  
172 of extremes: First, for each size class, a GEV model was fitted GEV using the block maxima

173 approach (Embrechts *et al.* 2008) by maximum likelihood as implemented in the functions *gev.fit*  
 174 from the {ismev} package (Port & Stephenson 2018) The relationship of the expected value ( $E[x]$ )  
 175 and variance ( $\text{Var}(x)$ ) with body size was evaluated *a posteriori* by means of linear regression.  $E[x]$   
 176 and  $\text{Var}(x)$  were estimated from the location ( $\mu$ ), scale ( $\sigma$ ) and shape ( $\xi$ ) parameters according to the  
 177 following equations:

$$\begin{aligned}
 E[x] &= \mu + \sigma \frac{(g_1 - 1)}{\xi} & \text{if } \xi \neq 0 \quad \xi < 1 \\
 E[x] &= \mu + \sigma \gamma & \text{if } \xi = 0 \\
 \text{Var}(x) &= \sigma^2 \frac{(g_2 - g_1^2)}{\xi^2} & \text{if } \xi \neq 0 \quad \xi < 1/2 \\
 \text{Var}(x) &= \sigma^2 \pi/6 & \text{if } \xi = 0
 \end{aligned}
 \tag{9}$$

179 where  $\gamma$  is Euler's constant and  $g_k = \Gamma(1 - k\xi)$  where  $\Gamma$  is the gamma function.

180 The second approach to fit GEV models was to unify in a single data frame weekly maximum  
 181 abundance per body size class, body size, average nutrients, average incident light, and average  
 182 water temperature as covariates and fit models by maximum likelihood using the function *fevd* from  
 183 the {extRemes} package (Gilleland & Katz 2016). We did not include covariates with significant  
 184 correlations in the same model in order not to inflate variance (see table 1 for model definition). We  
 185 fitted a set of nested models: a null model in which there was no dependence of GEV parameters  
 186 with any covariate (*e.g.*, size, DIN, etc.) and models following eq. 7 including size, nutrient or light  
 187 and the inverse of temperature effects in the GEV parameters. The inverse of temperature (in  
 188 Kelvin) was divided by the Boltzmann constant and so the estimate represent the activation energy  
 189 (E). Size class was used as a categorical covariate when associated to GEV shape parameter to  
 190 avoid convergence problems. Models that did not converged were not considered.

191 The use of the two statistical approaches ensured the use of all information, as resource  
 192 concentration (DIN) and incident light was not available for the whole time series. The data set with  
 193 resources and temperature were not available for the whole time series, it began in 2000 and ended  
 194 in 2011. Models were ranked using Akaike information criteria (AIC) and the smallest AIC chosen.

195 The selected model was inspected for residuals and goodness of fit using standard metrics (quantile-  
196 quantile plot and the distribution of residuals).

197

## 198 **RESULTS**

199 The total abundance of phytoplankton fluctuated along the year with maxima in summer and a  
200 tendency to decrease in winter, while temperature and DIN forms showed marked seasonal cycles  
201 (Fig. 2). A significant negative correlation between weekly average incident light and *in situ*  
202 measured DIN was found (Pearson's  $r = -0.75$ ,  $df = 437$ ,  $p = 2e^{-16}$ ). DIN concentration was limiting  
203 for all size classes, but the proportion of cases DIN was below  $k_s$  increased from the smallest size  
204 class to the largest size class (0.37, 0.42, 0.47, 0.52, 0.58, 0.67 and 0.82 from classes 5, 7, 9, 11, 13,  
205 15, and 17 in  $\log_2(\mu\text{m}^3 \text{org}^{-1})$ , respectively). Daily averaged incident light was always higher than  
206 the half-saturation constant for light.

207 GEV models were fitted for each size class. The expected value ( $E[x] = \log(\text{Abundance})$ ) showed a  
208 significant negative scaling with the logarithm of size class ( $\log_2(M)$ ). The linear model showed  
209 negative slope and a high coefficient of determination (Fig. 3A;  $E(x) = 9.68 - 0.82 \log_2(M)$ ;  $R^2 =$   
210  $0.74$ ;  $p < 0.01$ ;  $N = 6$ ). The 95% confidence interval of the slope was -1.38 to -0.26. The variance  
211 showed a humped pattern, increasing from the smallest size classes to the middle sizes classes, and  
212 then decreasing (Fig. 3B). The shape parameter (mean[standard error]) was negative in the smallest  
213 size classes ( $\xi = -0.25 [0.01]$ ) and closer to zero in larger size classes, indicating a tendency from  
214 Weibull to Gumbell distributions. Only size class 15 showed a positive shape parameter ( $\xi =$   
215  $0.066[0.02]$ ) indicative of Frechét distribution.

216 Under the second statistical approach, the model including the logarithm of size, nutrient  
217 concentration, the interaction between both and the inverse of temperature affecting location, the  
218 logarithm of size on scale and size and nutrients on shape parameters presented lower AIC with  
219 respect to the remaining models (model #0 in Table 1). The selected model showed that the fitted

220 coefficient representing the scaling of body size was negative ( $\mu_1 = -0.75$ ) and the logarithm of DIN  
221 presented a negative effect on location ( $\mu_2 = -0.52$ ) while the interaction between both was positive  
222 ( $\mu_3 = 0.017$ ). The inverse of temperature showed a negative scaling ( $\mu_4 = -0.58$ ) close to activation  
223 energy. Scale parameter showed a negative dependence with size ( $\sigma_1 = -0.265$ ). The shape was  
224 negative for all ( $\xi_i < 0$ ) except the larger size class ( $\xi_i > 0$ ). Residuals from the selected model  
225 showed a good fit to the data (Fig. 4). The results were congruent between the two statistical  
226 approaches employed.

227

## 228 **DISCUSSION**

229 We demonstrated the use of GEV theory to test an explicit hypothesis about the metabolic limits of  
230 maximum population density in phytoplankton. Using an extraordinary time series, we explored  
231 how metabolic limits to population abundance were shaped by body size and resources. The  
232 rigorous test of the metabolic limit to extreme population density using GEV theory opens a field  
233 for the analysis of extreme events in natural species-rich populations.

234

235 The use of the GEV approach is well developed in many fields, especially in hydrology and finance  
236 (Embrechts *et al.* 2008), but it is less explored in ecology (Katz *et al.* 2005; Batt *et al.* 2017).  
237 Assuming a Gaussian distribution of errors associated to the maximum abundance of species has  
238 been done (Belgrano *et al.* 2002; Cermeño *et al.* 2006), but it can lead to serious bias in the  
239 interpretation of results. The Gaussian distribution would lead to systematic bias in the estimation  
240 of the return periods, which is the average time between extreme events, an important metric for  
241 understanding the probability of occurrence of extreme events. For example, under a Gaussian  
242 model for the residuals, the return time of medium-sized phytoplankton organisms (size class 13 to  
243  $15 \sim 8000$  to  $32,700 \mu\text{m}^3 \text{org}^{-1}$ ) would yield 6 years to reach an extreme abundance of  $\sim 64 \text{ cells mL}^{-1}$ .  
244 <sup>1</sup>. In contrast, the estimated return time using the GEV approximation is 2 years. We remark that this

245 cell concentration represents a large amount of biomass of primary producers ( $5e^5$  to  $2e^6 \mu\text{m}^3 \text{mL}^{-1}$ ).  
246 Blooms of diatoms of intermediate size fuels aquatic food webs in temperate regions, channelling  
247 energy towards larger crustacean predators and ultimately fish, favouring the export of organic  
248 carbon (Widdicombe *et al.* 2010). The difference in the estimation of the return period between  
249 Gaussian and GEV approaches can have profound consequences for the understanding and  
250 managing of aquatic ecosystems, such as the estimation of harmful algal blooms. Appropriate  
251 characterization of the distribution of extreme values is therefore critical to forecast bloom  
252 formation and to track changes in the patterns induced by global change.

253 The limits imposed by metabolic restrictions to maximum population density are expected to  
254 operate in the dominant species (Lawton 1989). The use of the GEV theory to characterize this  
255 upper limit showed excellent performance. Under this framework, we were able to confirm the  
256 expected negative scaling of body size with extreme population abundance, supporting the  
257 hypothesis of metabolic restrictions, as found previously (Deng *et al.* 2012; Barneche *et al.* 2016).  
258 Moreover, the explicit inclusion of resources was instrumental to capture deviations from the  
259 expected size-abundance scaling value when resource are limiting (Enquist *et al.* 2007). Resource  
260 limitation could help to explain the otherwise contradictory evidence on size-density scaling  
261 presented in previous studies (e.g. Isaac *et al.* 2011). Deviations from the linear fit (Fig. 3) showed  
262 peaks coincident with the position of clumps detected for the planktonic community in this  
263 ecosystem (Segura *et al.* 2011), which suggests that other ecological forces are able to mould the  
264 pattern that arises from metabolic restrictions. Including the effects of ecological mechanisms and  
265 the role of resource co-limitation on the theoretical limits to population abundance is an interesting  
266 avenue to explore. Similarly, traits other than size (e.g. Silica wall in diatoms) can help to explain  
267 differences from the expected value caused by the limitation caused by other resources.

268 The GEV theory can provide further insight into the dynamics of natural populations. The Weibull  
269 distribution is the result of taking the maxima of a random variate that follows a bounded

270 distribution. The negative shape parameter representative of a Weibull distribution in small-sized  
271 populations is indicative of a strong population control of small sized organisms subjected to strong  
272 predator-prey interactions within the microbial food web (Calbet & Landry 2004) and consistent  
273 with a previous analysis of population fluctuations (Segura *et al.* 2013). However, medium-sized  
274 organisms showed higher variance (dictated by larger value of the scale parameter) and a shape  
275 parameter value close to zero, indicative of a Gumbel distribution. A Gumbel distribution in the  
276 logarithm of abundance ( $\log(N)$ ) implies that population abundance ( $N$ ) follows a *Fréchet*  
277 distribution, which is a fat tail distribution consistent to previous observations (Allen *et al.* 2001;  
278 Segura *et al.* 2013) and recent theoretical arguments (Segura & Perera 2019). This change in  
279 variance is mostly explained by the effect of the allometric scaling of the half-saturation constant,  
280 which exerts a stronger resource limitation to large-sized organisms when resources are limiting,  
281 but allows for a large increase in the upper limit when resources are not limiting. The scope for  
282 variability registered in medium- and large-sized organisms allows for outburst of abundance,  
283 thereby allowing escape from predatory control (Irigoien *et al.* 2005). The increase of abundance in  
284 medium-sized species fuels the herbivorous food web, where primary producers are fed upon by  
285 metazoan plankton consumed by large invertebrate or vertebrate predators (*e.g.*, fish larvae). This  
286 phenomenon has been described in temperate latitudes (Kjørboe 1993; Mann & Lazier 2006) and  
287 the English Channel (Widdicombe *et al.* 2010). Exploring these patterns beyond aquatic ecosystems  
288 could help to shed light on general principles regarding the size-structure and dynamics of natural  
289 populations.

290 Present results suggest nutrients and body size are two fundamental variables defining structure and  
291 variability of extreme abundance in the phytoplankton populations, and the most parsimonious  
292 model included size and nutrients but did not include temperature nor incident light (PAR; Table 1).  
293 However, the effect of light and temperature could not be discarded completely. First, there are  
294 significant correlations between the studied environmental variables (DIN, PAR, Temperature) that

295 render it difficult to tease out specific effects under this correlative approach. Experimental designs  
296 (*in vitro* or model-based) to isolate the effect of each variable could help delineate specific  
297 responses. The use of an invariant half-saturation constant for light dependence (López-Urrutia *et al.*  
298 *et al.* 2006) omit possible size dependences of light acquisition processes (Finkel *et al.* 2004; Mei *et al.*  
299 *et al.* 2009; Key *et al.* 2010). Theoretical size dependence of light acquisition (e.g. Mei *et al.* 2009)  
300 could be explicitly included in future model formulations to derive and test explicit predictions.  
301 Incident light reflects the amount of radiation reaching the water surface, while an underwater light  
302 environment is dependent on turbidity and depth of the thermocline which were not considered here  
303 (Huisman *et al.* 1999). Temperature is a key driver of metabolic processes (Brown *et al.* 2004), but  
304 it was not included in the selected model. Activation energy in primary producers is generally lower  
305 than in heterotrophic organisms (López-Urrutia *et al.* 2006; Segura *et al.* 2018), which implies a  
306 reduced impact on metabolic rates, together with the relatively cold and stable water temperature  
307 registered in the English Channel L4 station ( $T = 9\text{--}19\text{ }^{\circ}\text{C}$ ). The indirect effects of temperature may  
308 be more pronounced than its direct effect on metabolism. The changes in resource supply to the  
309 euphotic layer mediated by strong stratification or changes in the light landscape by deepening of  
310 the thermocline must be characterized. We showed that resource limitation is common for  
311 phytoplankton in the English Channel a pattern which could be greatly altered by human behaviour.  
312 Changes in thermal stratification and resource inflow to coastal zones caused by extreme weather  
313 effects (Smyth *et al.* 2010) are expected to increase in magnitude and frequency (Stockwell *et al.*  
314 2020), with marked effects in extreme population abundances.

315 In summary we tested explicit predictions on the scaling of the distribution of extreme population  
316 abundances of phytoplankton linking a well developed general extreme value theory with a  
317 metabolic resource limited model. We showed a marked effect of body size and resources in  
318 extreme population abundance and introduce a robust approach to explore community dynamics in  
319 natural species-rich ecosystems.

320 **Acknowledgements**

321 We thank Plymouth Marine Laboratory (PML) for generating and kindly providing data. We would  
322 like to thank Eric Gilleland for advise in fitting extreme models and suggestions in a previous  
323 version of the manuscript. We would like FVF for a grant to AMS and ANII for a grant to AMS  
324 (code FCE\_3\_2020\_1\_162710). SNI and PEDECIBA is also acknowledged for partial financial  
325 support. We also specially thank two reviewers for their constructive suggestions which greatly  
326 improved the manuscript.

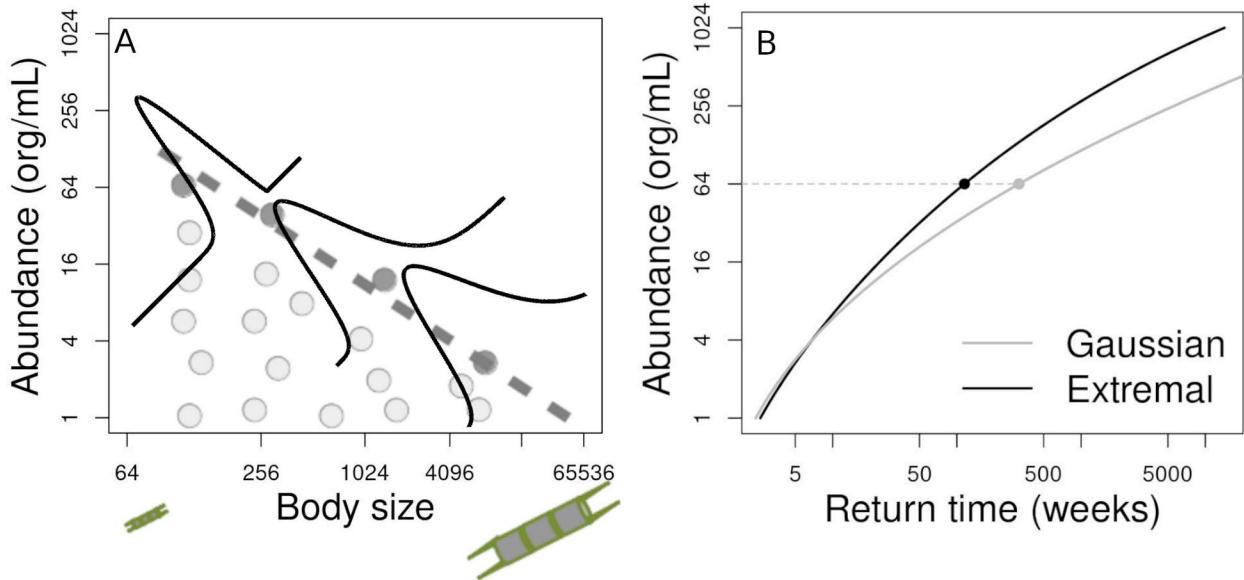
- Agustí, S., Duarte, C. & Kalff, J. (1987). Algal cell size and the maximum density and biomass of phytoplankton. *Limnol. Oceanogr.*, 32, 983–986.
- Aksnes, D.L. & Egge, J.K. (1991). A theoretical model for nutrient uptake in phytoplankton. *Marine Ecology Progress Series*, 70, 65–72.
- Allen, A.P., Li, B.-L. & Charnov, E.L. (2001). Population fluctuations, power laws and mixtures of lognormal distributions. *Ecology Letters*, 4, 1–3.
- Barneche, D.R., Kulbicki, M., Floeter, S.R., Friedlander, A.M. & Allen, A.P. (2016). Energetic and ecological constraints on population density of reef fishes. *Proceedings of the Royal Society B: Biological Sciences*, 283, 20152186.
- Batt, R.D., Carpenter, S.R. & Ives, A.R. (2017). Extreme events in lake ecosystem time series: Extreme events in lake ecosystem time series. *Limnol. Oceanogr.*, 2, 63–69.
- Belgrano, A., Allen, A.P., Enquist, B.J. & Gillooly, J.F. (2002). Allometric scaling of maximum population density: a common rule for marine phytoplankton and terrestrial plants. *Ecology letters*, 5, 611:613.
- Bjornstad, O.N. (2001). Noisy Clockwork: Time Series Analysis of Population Fluctuations in Animals. *Science*, 293, 638–643.
- Brown, J.H., Gillooly, J.F., Allen, A.P., Savage, V.M. & West, G.B. (2004). Toward a metabolic theory of ecology. *Ecology*, 85, 1771–1789.
- Calbet, A. & Landry, M.R. (2004). Phytoplankton growth, microzooplankton grazing, and carbon cycling in marine systems. *Limnol. Oceanogr.*, 49, 51–57.
- Cermeño, P., Marañón, E., Harbour, D. & Harris, R.P. (2006). Invariant scaling of phytoplankton abundance and cell size in contrasting marine environments. *Ecology Letters*.
- Deng, J., Zuo, W., Wang, Z., Fan, Z., Ji, M., Wang, G., *et al.* (2012). Insights into plant size-density relationships from models and agricultural crops. *Proceedings of the National Academy of Sciences*, 109, 8600–8605.
- Edwards, K.F., Thomas, M.K., Klausmeier, C.A. & Litchman, E. (2012). Allometric scaling and taxonomic variation in nutrient utilization traits and maximum growth rate of phytoplankton. *Limnology and Oceanography*, 57, 554–566.
- Embrechts, P., Klüppelberg, C. & Mikosch, T. (2008). *Modelling extremal events: for insurance and finance*. Stochastic modelling and probability. 4. corr. printing and 8. printing. Berlin.
- Enquist, B.J., Kerkhokoff, A.J., Stark, S.C., Swenson, N.G., McCarthy, M.C. & Price, C.A. (2007). A general integrative model for scaling plant growth, carbon flux, and functional trait spectra. *Ecology Letters*, 449.
- Finkel, Z.V., Irwin, A.J. & Schofield, O.M.E. (2004). Resource limitation alters the 3/4 size scaling of metabolic rates in phytoplankton. *Marine ecology progress series*, 273, 269–279.
- Gaines, S.D. & Denny, M.W. (1993). The Largest, Smallest, Highest, Lowest, Longest, and Shortest: Extremes in Ecology. *Ecology*, 74, 1677–1692.
- Gilleland, E. & Katz, R.W. (2016). extRemes 2.0: An Extreme Value Analysis Package in R. *Journal of Statistical Software*, 72, 1–39.
- Hatton, I.A., Dobson, A.P., Storch, D., Galbraith, E.D. & Loreau, M. (2019). Linking scaling laws across eukaryotes. *Proc Natl Acad Sci USA*, 116, 21616–21622.
- Huisman, J., Jonker, R.R., Zonnevel, C. & Weissing, J. (1999). Competition for light between phytoplankton species: experimental test of mechanistic theory. *Ecology*, 80, 211–222.
- Irigoiien, X., Flynn, K. & Harris, R. (2005). Phytoplankton blooms: a ‘loophole’ in microzooplankton grazing impact? *Journal of Plankton Research*, 27, 313–321.
- Isaac, N.J.B., Storch, D. & Carbone, C. (2011). Taxonomic variation in size-density relationships challenges the notion of energy equivalence. *Biology Letters*, 7, 615–618.

- Katz, R.W., Brush, G.S. & Parlange, M.B. (2005). Statistics of extremes: modeling ecological disturbances. *Ecology*, 86, 1124–1134.
- Keitt, T.H. & Stanley, H.E. (1998). Dynamics of North American breeding bird populations. *Nature*, 393, 257–260.
- Key, T., McCarthy, A., Campbell, D.A., Six, C., Roy, S. & Finkel, Z.V. (2010). Cell size trade-offs govern light exploitation strategies in marine phytoplankton. *Environmental Microbiology*, 12, 95–104.
- Kjørboe, T. (1993). Turbulence, Phytoplankton Cell Size, and the Structure of Pelagic Food Webs. In: *Advances in Marine Biology*. pp. 1–72.
- Lawton, J.H. (1989). What Is the Relationship between Population Density and Body Size in Animals? *Oikos*, 55, 429.
- López-Urrutia, A., San Martín, E., Harris, R.P. & Irigoien, X. (2006). Scaling the metabolic balance of the oceans. *Proceedings of the National Academy of Sciences of the United States of America*, 103, 8739–8744.
- Mann, K.H. & Lazier, J.R.N. (2006). *Dynamics Of Marine Ecosystems*.
- Marquet, P.A. (2005). Scaling and power-laws in ecological systems. *Journal of Experimental Biology*, 208, 1749–1769.
- May, R.M. (1973). *Stability and complexity in model ecosystems*. Princeton Landmarks in Biology. 2nd edn. London.
- Mei, Z.-P., Finkel, Z.V. & Irwin, A.J. (2009). Light and nutrient availability affect the size-scaling of growth in phytoplankton. *Journal of Theoretical Biology*, 259, 582–588.
- Port, O.S. functions written by J.E.H. with R. & Stephenson, R. documentation provided by A.G. (2018). *ismev: An Introduction to Statistical Modeling of Extreme Values*.
- Segura, A.M., Calliari, D., Kruk, C., Conde, D., Bonilla, S. & Fort, H. (2011). Emergent neutrality drives phytoplankton species coexistence. *Proceedings of the Royal Society B*, 278, 2355–2361.
- Segura, A.M. & Perera, G. (2019). The Metabolic Basis of Fat Tail Distributions in Populations and Community Fluctuations. *Frontiers in Ecology and Evolution*.
- Segura, A.M., Sarthou, F. & Kruk, C. (2018). Morphology-based differences in the thermal response of freshwater phytoplankton. *Biology Letters*.
- Segura, Calliari, D., Fort, H. & Lan, B.L. (2013). Fat tails in marine microbial population fluctuations. *Oikos*, 122, 1739–1745.
- Smyth, T.J., Fishwick, J.R., Al-Moosawi, L., Cummings, D.G., Harris, C., Kitidis, V., *et al.* (2010). A broad spatio-temporal view of the Western English Channel observatory. *Journal of Plankton Research*, 32, 585–601.
- Stockwell, J.D., Doubek, J.P., Adrian, R., Anneville, O., Carey, C.C., Carvalho, L., *et al.* (2020). Storm impacts on phytoplankton community dynamics in lakes. *Glob Change Biol*, 26, 2756–2784.
- Widdicombe, C.E., Eloire, D., Harbour, D., Harris, R.P. & Somerfield, P.J. (2010). Long-term phytoplankton community dynamics in the Western English Channel. *Journal of plankton research*, 32, 643–655.
- Widdicombe, C.E. & Harbour, D. (2021). Phytoplankton taxonomic abundance and biomass time-series at Plymouth Station L4 in the Western English Channel, 1992-2020.
- Woodward, E.M.S. & Harris, C. (2021). Micromolar Nutrient concentration profiles from the long term time series at Station L4 in the Western English Channel from 2000 to 2020.
- Zaoli, S., Giometto, A., Maritan, A. & Rinaldo, A. (2017). Covariations in ecological scaling laws fostered by community dynamics. *Proceedings of the National Academy of Sciences*, 114, 10672–10677.

328 Table 1.- Generalized Extreme Value (GEV) distribution models fitted to phytoplankton maximum  
 329 population density in the English channel L4 station. Body size (logM) was fitted as a continuous  
 330 covariate and also as a categorical covariate (classM) where subscript  $i$  denotes a specific parameter  
 331 for each size class. The model following eq. 7 including the logarithm of Dissolved Nitrogen  
 332 Concentration (logDIN) and Incident light (PAR) improved model fitting as evidenced by the  
 333 lowest AIC ( $\Delta$ AIC) and did not showed convergence problems. The “interaction” between the two  
 334 additive variables in the location parameter is showed (interaction).

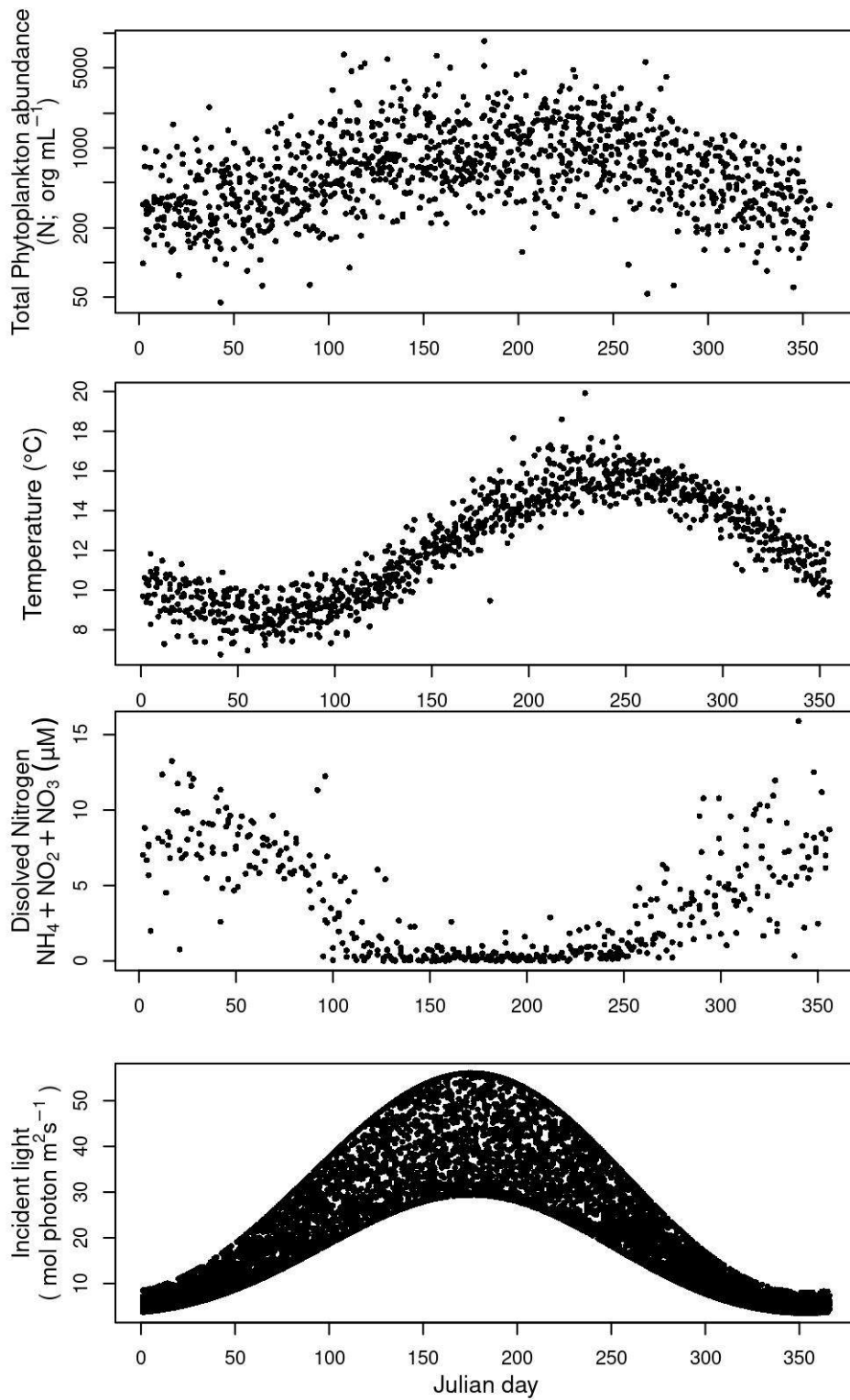
#	Location ( $\mu$ )	Scale ( $\sigma$ )	Shape ( $\xi$ )	$\Delta$ AIC
0	$\mu + \mu_1 \log M + \mu_2 \log \text{DIN} + \mu_3 \text{interaction} + \mu_4 \text{invTemp}$	$\sigma + \sigma_1 \log M$	$\xi + \xi_2 \log \text{DIN} + \xi_i \text{classM}$	0
1	$\mu$	$\sigma$	$\xi$	2021
2	$\mu + \mu_1 \log M$	$\sigma + \sigma_1 \log M$	$\xi$	619
3	$\mu + \mu_1 \log M$	$\sigma + \sigma_1 \log M$	$\xi$	376
4	$\mu + \mu_1 \log M$	$\sigma + \sigma_1 \log M$	$\xi + \xi_i \text{classM}$	168
5	$\mu + \mu_1 \log M + \mu_2 \log \text{DIN} + \mu_3 \text{interaction}$	$\sigma + \sigma_1 \log M$	$\xi + \xi_2 \log \text{DIN} + \xi_i \text{classM}$	13
6	$\mu + \mu_1 \log M + \mu_2 \text{invTemp}$	$\sigma + \sigma_1 \log M$	$\xi + \xi_i \text{classM}$	98
7	$\mu + \mu_1 \log M + \mu_2 \log \text{DIN} + \mu_3 \text{interaction}$	$\sigma + \sigma_1 \text{invTemp}$	$\xi + \xi_i \text{classM}$	431

335



336

337 Figure 1.- Schematic representation of the A) Size abundance distribution showing two patterns: i)  
 338 the expected negative relationship (grey dashed line with negative slope) and ii) the generalized  
 339 extremal distribution (GEV) expected in each size class for the residuals of taking the weekly  
 340 maxima (darkgrey dots) of species abundance (grey dots). B) the average time to observe (*i.e.* return  
 341 time) an extreme event differ importantly between using the appropriate GEV distribution and  
 342 assuming a Gaussian approximation. Note axis are in logarithmic scale.

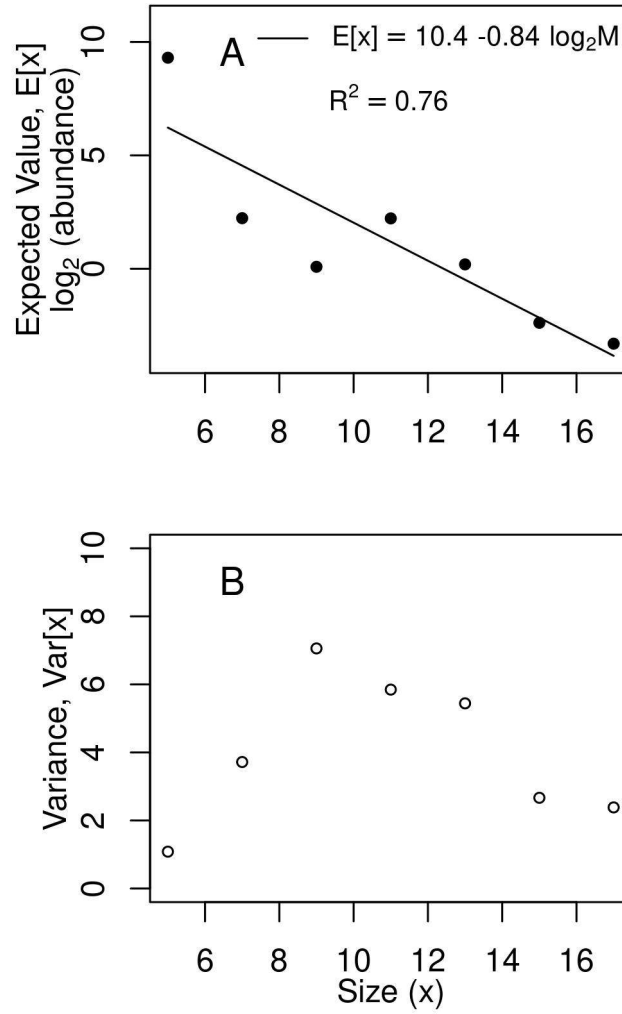


343

344 Figure 2.- Temporal dynamics of phytoplankton abundance, temperature, nutrients and incident  
 345 light measured in the English channel L4 station from 1992 to 2009.

346

347

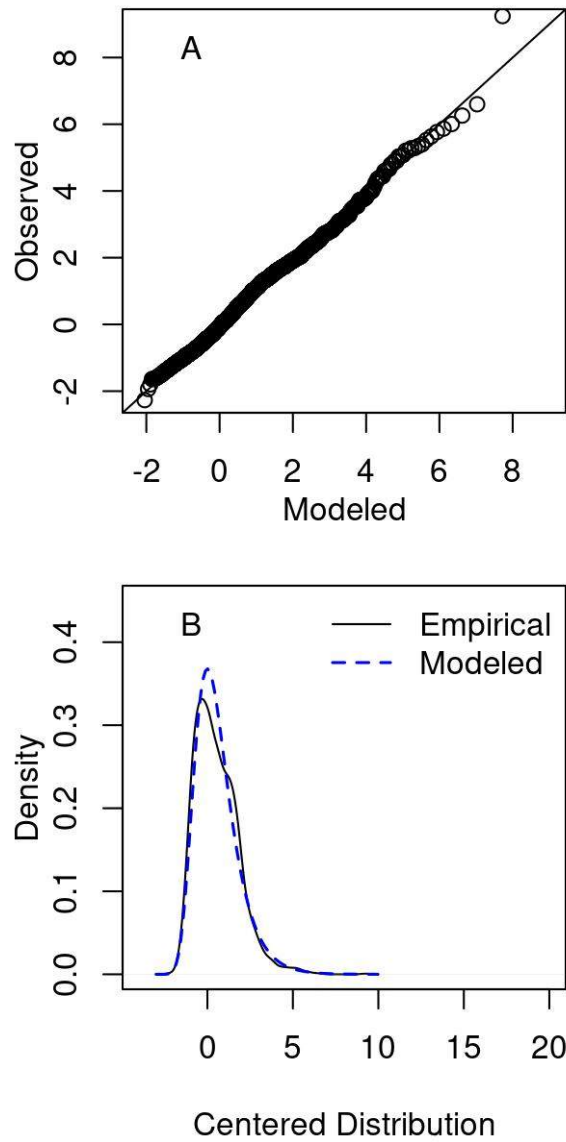


349

350 Figure 3.- Size scaling of the A) expected value ( $E[x]$ ) and B) the variance ( $\text{Var}[x]$ ) of the fitted  
 351 GEVs distributions. The value of the negative relationship (Average [95%CI]= -0.84 [-1.38–0.30])  
 352 between size and the expected value supports the theoretical predictions of a negative scaling  
 353 related to metabolism. Phytoplankton size classes are in logarithmic classes (in log<sub>2</sub>).

354

355



356

357

358

359

360

361

Figure 4.- Summary plots for the best fitted GEV model (#0 in Table 1 in agreement with theoretical eq. 7) with size, resources and the inverse of temperature as covariates to explain maximum population abundance data in the L4 station in the English channel. A) quantile-quantile plot and B) residual density in the observed and modelled data.